Myocardial blood flow determination from contrast-free magnetic resonance imaging quantification of coronary sinus flow

Tingsgaard, Jakob Koefoed; Sørensen, Martin Heyn; Bojer, Annemie Stege; Anderson, Robert H.; Broadbent, David Andrew; Plein, Sven; Gæde, Peter; Madsen, Per Lav

Published in:
Journal of Magnetic Resonance Imaging

DOI:
10.1002/jmri.28919

Publication date:
2024

Document version:
Accepted manuscript

Citation for pulished version (APA):
Tingsgaard, J. K., Sørensen, M. H., Bojer, A. S., Anderson, R. H., Broadbent, D. A., Plein, S., Gæde, P., & Madsen, P. L. (2024). Myocardial blood flow determination from contrast-free magnetic resonance imaging quantification of coronary sinus flow. *Journal of Magnetic Resonance Imaging*, *59*(4), 1258-1266. https://doi.org/10.1002/jmri.28919

Tingsgaard Jakob (Orcid ID: 0000-0002-5589-6268)
Broadbent David (Orcid ID: 0000-0002-5892-4762)

Myocardial blood flow determination from contrast-free MRI quantification of coronary sinus flow

Abstract

Background: Determination of myocardial blood flow (MBF) with MRI is usually performed with dynamic contrast enhanced imaging (MBF_{DCE}). MBF can also be determined from coronary sinus blood flow (MBF_{CS}), which has the advantage of being a non-contrast technique. However, comparative studies of MBF_{DCE} and MBF_{CS} in large cohorts are lacking.

Purpose: To compare MBF_{CS} and MBF_{DCE} in a large cohort.

Study type: Prospective, sequence-comparison study.

Population: 147 patients with type 2 diabetes mellitus (age: 56+/-12 years; 106 male; diabetes duration: 12.9 +/- 8.1 years), and 25 age-matched controls.

Field strength/sequences: 1.5 Tesla scanner. Saturation recovery sequence for MBF_{DCE} vs. phase-contrast gradient-echo pulse sequence (free-breathing) for MBF_{CS}.

Assessment: MBF_{DCE} and MBF_{CS} were determined at rest and during coronary dilatation achieved by administration of adenosine at 140 µg/kg/min. Myocardial perfusion reserve (MPR) was calculated as the stress/rest ratio of MBF values. Coronary sinus flow was determined twice in the same imaging session for repeatability assessment.

Statistical tests: Agreement between MBF_{DCE} and MBF_{CS} was assessed with Bland and Altman´s technique. Repeatability was determined from single-rater random intra-class and repeatability coefficients.

This is the author manuscript accepted for publication and has undergone full peer review but has not been through the copyediting, typesetting, pagination and proofreading process, which may lead to differences between this version and the Version of Record. Please cite this article as doi: 10.1002/jmri.28919

Results: Rest and stress flows, including both MBF_{DCE} and MBF_{CS} values, ranged from 33 to 146 mL/min/100g and 92 to 501 mL/min/100g, respectively. Intra-class and repeatability coefficients for MBF_{CS} were 0.95 (CI 0.90;0.95) and 5 mL/min/100g. In Bland-Altman analysis, mean bias at rest was – 1.1mL/min/100g (CI -3.1;0.9) with limits of agreement of -27 and 24.8 mL/min/100g. Mean bias at stress was 6.3 mL/min/100g (CI -1.1;14.1) with limits of agreement of -86.9 and 99.9. Mean bias of MPR was 0.11 (CI: -0.02;0.23) with limits of agreement of -1.43 and 1.64.

Conclusion: MBF may be determined from coronary sinus blood flow, with acceptable bias, but relatively large limits of agreement, against the reference of MBF_{DCE}.

Key-words: dynamic contrast enhanced imaging, coronary sinus, coronary sinus blood flow, myocardial blood flow, cardiac veins.

Introduction

The myocardium relies on a constant blood supply, and quantification of left ventricle (LV) myocardial blood flow (MBF) is increasingly recognized as being important in non-ischaemic cardiomyopathy (1). It may also be of prognostic relevance in ischaemic heart disease as prognosis is related to the total myocardial LV ischaemia, which can be assessed with global MBF estimates (1). MBF can be quantified non-invasively with positron emission tomography or MRI. With both modalities, this conventionally requires the administration of contrast agents, specifically radioisotopes or gadolinium-chelates, respectively (2,3). Positron emission tomography determination of MBF is associated with a radiation dose comparable to a calcium score CT scan of the heart, and determination of MBF from MRI dynamic contrast enhanced imaging (MBF_{DCE}) is contraindicated in patients with low glomerular filtration rate (4–6).

It would be desirable to determine MBF without the use of intravenous contrast agents. An alternative method for quantification of global MBF is to measure the venous outflow of the myocardium in the coronary sinus (MBF_{CS}) (7). Anatomical studies suggest that the vast majority of the LV myocardium is drained via the greater cardiac venous system, eventually draining into the coronary sinus (7,8). Originating from the junction between the oblique vein of the LA and the great cardiac vein, the coronary sinus is a venous vessel with a diameter of approximately 10 mm (9). It extends within the left atrioventricular groove until it empties into the right atrium (7,8,10). The great cardiac vein drains the majority of the anterior part of the ventricles, along with one to two thirds of the muscular ventricular septum (9). It contributes over two-thirds of coronary sinus blood flow (9,11). Further contributions come from the middle cardiac vein, which drains the diaphragmatic parts of the ventricles and the inferior part of the muscular septum, the small cardiac vein, which drains the inferior and

lateral parts of the right ventricle, and the left marginal vein, which drains the lateral part of the LV (9). MBF_{CS} should thus approximate global MBF (12–14). Flow-sensitive pulse sequences (phase contrast) which are standard on any MR scanner, are performed without contrast, and routinely only take 1-2 minutes to perform, making this method both less time consuming and safe for patients with low kidney function.

Small validation studies on the use of MBF_{CS} have been performed using phantom models (15); animal experimental models with flow probes (16); and in groups of 12-20 normal subjects and patients with myocardial ischaemia as compared to MBF from positron emission tomography (17,18), where they co-vary linearly both during rest and adenosine-stress. Other studies have shown that MBF_{CS}-derived myocardial perfusion reserve (MPR), the ratio of MBF during maximal coronary vasodilatation to rest MBF, correlates with myocardial ischemia as assessed by MBF_{DCE} and is associated with adverse prognosis at 3.5 years (19–23). Larger cohort studies on the agreement of MBF_{CS} and MBF_{DCE}, however, including those in patients with lowered MBF as determined by a reference standard technique, are lacking.

Thus, the aim of this study was to compare dynamic contrast enhanced imaging and coronary sinus flow assessment of MBF and MPR in a large cohort of patients with type 2 diabetes mellitus (T2DM) and 25 normal age-matched controls.

Methods and patients

Study population

Our study complies with the declaration of Helsinki, and was approved by the local ethics committee (SJ-490). All participants gave written, informed consent. Patients were recruited from the outpatient clinic at the department of endocrinology at Naestved-Slagelse Regional

Hospital from January 2016 to March 2018. Patients aged from 18 to 80 years, and diagnosed with T2DM for at least three months, were eligible to participate in the study. We excluded patients if they had severe claustrophobia, more than trivial paroxysmal atrial fibrillation, glomerular filtration rates of less than 30 ml/min/m^2, implanted cardiac devices, cochlear implants, or other contraindications to MRI or to adenosine. Patients were also excluded if the obtained images were of insufficient quality, which was determined by the two analysts assessing the scans. Patients with previous coronary arterial bypass surgery, or with symptoms of typical anginal chest pain were also excluded from the study, since its main objective was to describe phenotypical changes to the heart in the setting of T2DM. We also included 25 healthy sex and age matched subjects without T2DM or coronary arterial disease.

Study design

The protocol has been described in detail in a previous study (24). In short, the study was designed as a prospective MRI cross-sectional survey of patients with T2DM in order to characterize cardiac phenotypic changes. Any pertinent history of diabetic complications, hypertension, coronary arterial disease, and medication was retrieved from the electronic patient journal or from the patients themselves. A positive history of hypertension was defined as a resting blood pressure higher than 140/90 mmHg, an active prescription of antihypertensive medication, or a positive confirmation from the patient. A positive history of ischaemic heart disease was defined as previous acute myocardial infarction, angiographically verified coronary stenosis, or ischaemic lesions noted on late gadolinium enhancement images.

MRI Protocol

All participants were instructed to refrain from caffeine consumption for 24 hours prior to the scan. MRI was performed on a 1.5T scanner (Siemens Avanto; Siemens, Erlangen, Germany) with spine- and surface coils, retrospective ECG gating, and with patients in the supine position. Anatomical images were acquired during breath-hold at end-expiration. Following scout images, LV function was evaluated via cardiac short axis stack (SAX) of images covering the base to apex of the heart using a balanced steady-state free precession cine imaging sequence; representative parameters: TE 1.25ms, TR 49.81ms, 16 segments per cardiac phase, echo spacing 3.3ms, flip-angle 80°, slice thickness 8mm, matrix 168x208, output 25 reconstructed phases per cardiac cycle.

An intravenous infusion of adenosine, at 140 µg/kg/min, was administered for 3 minutes before starting perfusion recordings; in total adenosine was administered for 4.5-5 minutes. The stress perfusion images were obtained first and the coronary sinus flow sequences were obtained immediately after. Perfusion and coronary sinus flow sequences were then repeated more than 10 minutes later at rest. Gadobutrol (Gadovist®, Bayer AG, Germany) was administered (.075 mmol/kg) at a rate of 5 ml/s, followed by 20 ml of normal saline for both stress and rest perfusion imaging. Acquisition time depended on heart rate but ranged from 30 to 45 seconds. Myocardial perfusion images were obtained from three subset SAX slices (basal, mid-ventricular and apical) using a saturation recovery sequence with spoiled gradient echo readout (TE 1.1ms, TR 162.25ms, SR 100ms, flip angle 12°, slice thickness 10mm, matrix 144x160, FOV 342x380, echo spacing 2.7ms, number of segments 49).

T1 maps were acquired during breath-hold in 3 short-axis slices matching the slice position of perfusion sequences, using a Shortened Modified Look-Locker Inversion recovery

(ShMOLLI) sequence (TR 279.8ms, TE 1.13ms, flip angle 35º, slice thickness 8 mm, spatial resolution 1.98x1.98 mm, matrix 144x256). Native T1 mapping was performed prior to the stress perfusion sequence and post- contrast T1 mapping was carried out a minimum of 10 minutes after the first contrast injection and just before the rest perfusion sequence.

For MBF_{CS}, the coronary sinus was identified in the 2-chamber view (Fig. A). Blood-flow through the sinus was determined with a free-breathing phase-contrast gradient-echo pulse sequence (TE 3.8 ms, TR 13.4 ms, segments 6, FOV 240–320 mm, matrix 77 × 128, number of reconstructed phases per cardiac cycle 25, number of excitations 1, slice thickness 6 mm) with initial velocity encoding of 0.5 m/s, with 20% up-ward adjustment of velocity encoding if signs of aliasing were noted (Fig. B). When time allowed, and with the patient still in the scanner, the flow-sequence was repeated to determine intra-study reproducibility of coronary sinus flows at rest. Heart rate and blood pressure were recorded at baseline and during adenosine infusion. Ten minutes after the resting perfusion contrast injection, delayed gadolinium enhancement images were acquired covering the LV base to apex using SAX matching the cine SAX stack, and in the LAX 2-, 3- and 4-chamber views with magnitude-only and phase sensitive inversion recovery reconstruction sequences (TE 1.3 ms; TI 2.8 ms; Inversion time 250-300 ms; matrix 256 x 128; parallel imaging factor 2; breath-hold duration 2 heart beats/slice).

Data analysis

LV volumes, mass, and ejection fraction and coronary sinus blood flow were calculated with third-party software (Circle Cardiovascular Imaging Inc., Calgary Canada, v. 5.5.1) by semi-automatic tracing of the endocardial and epicardial contours in end diastolic and end systolic phases. Analyses of cardiovascular parameters were performed by two readers independently.

Both with more than 3 years of cardiac MRI experience. The LA maximal volume was manually traced in the LV end-systolic frame. Coronary sinus flow was determined from flow-sequences. Quantification of MBF_{DCE} was performed for the mid-slice perfusion data using a tool developed in MATLAB 2015b (MathWorks, Nattick, MA, USA) (25),(24). In this current study, all patients, including those with fibrosis, were included. Regions of interest were drawn in the LV blood pool in both the perfusion images and T_1 map. The non-linear response of signal intensity to contrast agent concentration was corrected based on the baseline signal intensity and T_1 data (25). Data were cropped to the end of the first-pass. Fermi-constrained deconvolution was performed to yield segmental MBF estimates (26) and whole heart MBF_{DCE} was determined from the average of segmental MBF and the myocardial volume.

Statistical analysis

Continuous variables are presented as mean ± SD and categorical variables as absolute values and percentages. MBF_{DCE} and MBF_{CS} were indexed to each 100 g of myocardial mass as determined from the short axis cine image stack. MPR was calculated by dividing MBF_{DCE}, or coronary sinus flow, during stress with MBF_{DCE}, or coronary sinus flow, during rest. Co-variation of MBF_{DCE} and MBF_{CS} was analysed with the Bland and Altman technique and linear regression models of the two (coefficient of determination, R^2). Determinations were made for rest and adenosine stress values as well as for the increments with stress, and the MPR. Reproducibility of MBF_{CS} was determined by calculating the repeatability coefficient along with the intra class coefficient (ICC) as suggested by Bland and Altman (27). All calculations were made with R-Studio version 3.6.3 (2019-12-12). A p-value < 0.05 was considered statistically significant.

Results

For the overall T2DM study, 423 patients were initially approached. Eighty-one patients had one or more criteria for exclusion, and further 95 declined to participate, leaving 247 patients. 9 patients had scans of insufficient quality while 45 scans were discontinued by the patients mainly due to claustrophobia and back-pain. In total, therefore, 193 patients with T2DM, and 25 controls matched for age and sex, were included in the study. In 147 of these patients and all 25 normal controls, both MBF_{DCE} and MBF_{CS} were available.

Patient characteristics, including complications from DM and MRI measurements, are given in Tables 1 and 2. MBF_{DCE} values in the normal subjects ranged from a lowest rest value of 43 mL/min/100g to a maximal stress value of 494 mL/min/100g, and in the patients with T2DM from a lowest rest value of 39 mL/min/100g to a maximal stress value of 501 mL/min/100g (Fig. B). At rest, both MBF_{DCE} and MBF_{CS} were significantly higher in patients with T2DM than in controls. With stress, however, MBF_{DCE} and MBF_{CS} were both significantly lower in patients with T2DM than in controls (Table 2 and Fig. B).

In normal subjects, resting and stress MBF_{CS} were on average 8.4 mL/min/100g and 24.7 ml/min/100 g higher than MBF_{DCE} amounting to 113% and 112% of MBF_{DCE}, respectively. In patients with T2DM, resting and stress MBF_{CS} were on average 0.2 mL/min/100g and 12.6 ml/min/100g lower than MBF_{DCE} amounting to 100% and 97% of MBF_{DCE}, respectively. Simple linear regression showed that $MBF_{DCE} = 13.8+0.8*MBF_{CS}$ at rest (R^2 0.56); $MBF_{DCE} = 22.4+0.9*MBF_{CS}$ at stress (R^2 0.74); $MBF_{DCE} = 18.8+0.9*MBF_{CS}$ for the increment values (R^2 0.77); and $MPR_{DCE} = 0.6+0.9*MPR_{CS}$ for the MPR (R^2 0.72). In the 46 T2DM patients in whom repeat rest MBF_{CS} measurements were made, the intra-class

and repeatability coefficients for MBF_{CS} were 0.95 (CI 0.90; 0.95) and 5.2 mL/min/100g, respectively.

Including all subjects, MBF_{DCE} and MBF_{CS} increased during adenosine-stress, with mean absolute increments of 172 and 163 mL/min/100g, and with mean MPR of 3.35 and 3.24, respectively.

Bland-Altman plots including all subjects showed that MBF_{DCE} and MBF_{CS} co-varied with a small bias, but with limits of agreement of 40-45% (Fig. D). The mean bias of MBF measurements during rest was 1.1mL/min/100g (CI -3.1;0.9) with limits of agreement of -27 (CI -30.5; -23.5) and 24.8 (CI 21.3; 28.3) mL/min/100g. Increase from rest-to-stress was 6 (CI -1; 14) mL/min/100g, with corresponding limits of agreement of 93 (CI 81; 105) and -80 (CI -93; 68) mL/min/100g, and the mean bias of stress-reserve was 0.11 (CI: -0.02; 0.23) with corresponding limits of agreement of -1.43 (CI -1.65; -1.21) and 1.64 (CI 1.42; 1.86).

Bland-Altman plots within each subject group (diabetic and control) showed that mean MBF_{DCE} and MBF_{CS} covaried with a small bias but with limits of agreement ranging from 24.5-60.5%. Within the diabetic and the control cohort mean bias range were 0.14-5.4% and 1.04-10.5% respectively (fig E and fig F). Limits of agreement ranged from 27-60.5% (diabetic cohort) and 24.5-59.2% (control cohort), fig. E and fig. F respectively.

Discussion

This study assessed the degree to which MBF as measured by coronary sinus blood flow (MBF_{CS}) reflects MBF determined by dynamic contrast enhanced imaging (MBF_{DCE}) in a large cohort of patients with type 2 diabetes and age-matched normal controls (Fig. C).

Our findings show that MBF_{DCE} and MBF_{CS} co-vary with a small mean bias from rest to stress, but with relatively large limits of agreement. The study also showed that it was

possible to reproduce measurements of MBF_{CS}. MBF_{CS} therefore reflect MBF_{DCE}, as both the mean bias of MBF_{CS} compared to $MBF_{DCE,}$ and the repeatability coefficient of MBF_{CS} were small. Dividing the cohort into a diabetic group and a control group did not alter the mean bias dramatically. Bland-Altman plots showed low mean bias both within the diabetic and control cohorts, with relatively large limits of agreement in both. While mean biases were small, limits of agreement in this study, however, were large. Their importance must be taken into consideration for the specific research situation in question. MBF determined with contrast enhanced MRI is considered a non-invasive reference technique, with high co-variation to MBF as determined with positron emission tomography (18,28) and invasive FFR (29).

In the study patients with myocardial fibrosis were included but segments with fibrosis from previous myocardial infarction or visually detectable significant perfusion defects were excluded from analysis. Studies have shown that in patients myocardial fibrosis MBF_{CS} and MBF_{DCE} are reduced during stress (30,31).

Venous drainage of the LV myocardium occurs largely via the coronary sinus (8). Anomalies of the coronary sinus itself are uncommon, but some variation of tributary veins is seen (7,9). Except for the study of Ganz et al. (11) with retrogradely placed thermodilution flow-probes in the coronary sinus and great cardiac vein, studies quantifying the relative contribution to the total MBF from each territory of venous drainage are scarce. Nevertheless, it is reasonable to consider the coronary sinus flow as a parameter for the venous blood flow from the LV. Our study demonstrates that, in a wide range of MBFs, MBF_{DCE} and MBF_{CS} are on average equal. A major strength of our study is that it includes a large number of patients with widely ranging MBF_{DCE} and MBF_{CS}. Hence, even without precise mapping of tributary veins to the

coronary sinus, it is possible to report that MRI-determination of coronary sinus flow may discern low from normal values of MBF.

Limitations

A notable limitation of our study was the lack of mapping of tributary veins to the coronary sinus. In the individual subject, therefore, we do not know if small and middle cardiac veins were connecting to the coronary sinus up- or downstream to the scan plane. From anatomical considerations, we would expect that, in most patients, the middle and small cardiac veins would insert into the coronary sinus down-stream from the applied coronary sinus measurement site. If, in some subjects, they may have inserted up-stream, this would contribute to a higher MBF_{CS} than MBF_{DCE}. The small cardiac vein, however, mostly inserts into the coronary sinus, and usually in the very last portion of the coronary sinus (8). Hence, right ventricle myocardial flow drained via the small cardiac vein is probably excluded from the MBF_{CS} determination in most, if not all, subjects. On the other hand, additional contribution from the right ventricle myocardium may explain why, in some cases, the MBF_{CS} was higher than the MBF_{DCE}. In line with this, in some subjects we speculate that a higher proportion of venous drainage of the LV myocardium is via small veins emptying directly into the LV cavity. This would account for a higher MBF_{DCE} than MBF_{CS}. Pre-examination of the precise coronary sinus and tributary vein anatomy with MR or CT may improve co-variation of MBF_{CS} and MBF_{DCE}.

A further limitation of this study was that gadolinium administration precluded inclusion of patients with eGFR below 30 ml/min/1.73m^2. We cannot report, therefore, on patients with impaired kidney function, in whom the co-variation of MBF_{CS} and MBF_{DCE} may in theory be different. Further, our study is limited to assess intra-observer variability and has not reassessed MBF_{DCE} and MBF_{CS} on separate days or with repositioning of the patient.

Conclusion

As compared to the non-invasive reference technique of dynamic contrast enhanced imaging, myocardial blood flow can be determined with a small bias using the non-contrast technique of flow-velocity encoded imaging across the coronary sinus. Reproducibility testing was very limited but promising. Limits of agreement, however, are relatively large and must considered for each specific research or clinical question.

Conflict of interest

Nothing to disclose.

Funding

No funding.

Sample Data Availability Statements

Data available on request

References

1. Murthy VL, Bateman TM, Beanlands RS, et al. Clinical Quantification of Myocardial Blood Flow Using PET: Joint Position Paper of the SNMMI Cardiovascular Council and the ASNC. J Nucl Med Off Publ Soc Nucl Med. 2018;59(2):273–93.

2. Pelletier-Galarneau M, Martineau P, El Fakhri G. Quantification of PET Myocardial Blood Flow. Curr Cardiol Rep. 2019 28;21(3):11.

3. Jerosch-Herold M. Quantification of myocardial perfusion by cardiovascular magnetic resonance. J Cardiovasc Magn Reson. 2010 12(1):57.

4. Case JA, deKemp RA, Slomka PJ, Smith MF, Heller GV, Cerqueira MD. Status of cardiovascular PET radiation exposure and strategies for reduction: An Information Statement from the Cardiovascular PET Task Force. J Nucl Cardiol. 2017 1;24(4):1427–39.

5. Sabarudin A, Siong TW, Chin AW, Hoong NK, Karim MKA. A comparison study of radiation effective dose in ECG-Gated Coronary CT Angiography and calcium scoring examinations performed with a dual-source CT scanner. Sci Rep. 20190313;9(1).

6. Thomsen HS, Morcos SK, Almén T et al. Nephrogenic systemic fibrosis and gadolinium-based contrast media: updated ESUR Contrast Medium Safety Committee guidelines. Eur Radiol. 2013 ;23(2):307–18.

7. Sirajuddin A, Chen MY, White CS, Arai AE. Coronary venous anatomy and anomalies. J Cardiovasc Comput Tomogr. 2020;14(1):80–6.

8. Loukas M, Bilinsky S, Bilinsky E, el-Sedfy A, Anderson RH. Cardiac veins: a review of the literature. Clin Anat N Y N. 2009;22(1):129–45.

9. Kassem MW, Lake S, Roberts W, Salandy S, Loukas M. Cardiac veins, an anatomical review. Transl Res Anat. 2021;23:100096.

10. Anderson RH, Spicer DE, Hlavacek AM, Cook AC, Backer CL. Wilcox's Surgical Anatomy of the Heart. 4th ed. Cambridge University Press; 2013.

11. Ganz W, Tamura K, Marcus HS, Donoso R, Yoshida S, Swan HJ. Measurement of coronary sinus blood flow by continuous thermodilution in man. Circulation. 1971 ;44(2):181–95.

12. Bloch KM, Carlsson M, Arheden H, Ståhlberg F. Quantifying coronary sinus flow and global LV perfusion at 3T. BMC Med Imaging. 2009 11;9:9.

13. Dandekar VK, Bauml MA, Ertel AW, Dickens C, Gonzalez RC, Farzaneh-Far A. Assessment of global myocardial perfusion reserve using cardiovascular magnetic resonance of coronary sinus flow at 3 Tesla. J Cardiovasc Magn Reson Off J Soc Cardiovasc Magn Reson. 2014 27;16(1):24.

14. van Rossum AC, Visser FC, Hofman MB, Galjee MA, Westerhof N, Valk J. Global left ventricular perfusion: noninvasive measurement with cine MR imaging and phase velocity mapping of coronary venous outflow. Radiology. 1992;182(3):685–91.

15. Arheden H, Saeed M, Törnqvist E et al. Accuracy of segmented MR velocity mapping to measure small vessel pulsatile flow in a phantom simulating cardiac motion. J Magn Reson Imaging JMRI. 2001;13(5):722–8.

16. Lund GK, Wendland MF, Shimakawa A et al. Coronary sinus flow measurement by means of velocity-encoded cine MR imaging: validation by using flow probes in dogs. Radiology. 2000;217(2):487–93.

17. Schwitter J, DeMarco T, Kneifel S et al. Magnetic resonance-based assessment of global coronary flow and flow reserve and its relation to left ventricular functional parameters: a comparison with positron emission tomography. Circulation. 2000 Jun;101(23):2696–702.

18. Koskenvuo JW, Sakuma H, Niemi P et al. Global myocardial blood flow and global flow reserve measurements by MRI and PET are comparable. J Magn Reson Imaging JMRI. 2001;13(3):361–6.

19. Kato S, Fukui K, Saigusa Y et al. Coronary Flow Reserve by Cardiac Magnetic Resonance Imaging in Patients With Diabetes Mellitus. JACC Cardiovasc Imaging. 2019;12(12):2579–80.

20. Kato S, Saito N, Nakachi T et al. Stress Perfusion Coronary Flow Reserve Versus Cardiac Magnetic Resonance for Known or Suspected CAD. J Am Coll Cardiol. 2017 15;70(7):869–79.

21. Herring N, Tapoulal N, Kalla M et al. Neuropeptide-Y causes coronary microvascular constriction and is associated with reduced ejection fraction following ST-elevation myocardial infarction. Eur Heart J. 2019;40(24):1920–9.

22. Nakamori S, Sakuma H, Dohi K et al. Combined Assessment of Stress Myocardial Perfusion Cardiovascular Magnetic Resonance and Flow Measurement in the Coronary Sinus Improves Prediction of Functionally Significant Coronary Stenosis Determined by Fractional Flow Reserve in Multivessel Disease. J Am Heart Assoc. 2018;7(3).

23. Shomanova Z, Florian A, Bietenbeck M, Waltenberger J, Sechtem U, Yilmaz A. Diagnostic value of global myocardial perfusion reserve assessment based on coronary sinus flow measurements using cardiovascular magnetic resonance in addition to myocardial stress perfusion imaging. Eur Heart J Cardiovasc Imaging. 2017;18(8):851–9.

24. Sørensen MH, Bojer AS, Broadbent DA, Plein S, Madsen PL, Gæde P. Cardiac perfusion, structure, and function in type 2 diabetes mellitus with and without diabetic complications. Eur Heart J Cardiovasc Imaging. 2020;21(8):887–95.

25. Biglands J, Magee D, Boyle R, Larghat A, Plein S, Radjenović A. Evaluation of the effect of myocardial segmentation errors on myocardial blood flow estimates from DCE-MRI. Phys Med Biol. 2011;56(8):2423–43.

26. Jerosch-Herold M, Wilke N, Stillman AE. Magnetic resonance quantification of the myocardial perfusion reserve with a Fermi function model for constrained deconvolution. Med Phys. 1998;25(1):73–84.

27. Bland JM, Altman DG. Measuring agreement in method comparison studies. Stat Methods Med Res. 1996;8(2).

28. Bratis K, Mahmoud I, Chiribiri A, Nagel E. Quantitative myocardial perfusion imaging by cardiovascular magnetic resonance and positron emission tomography. J Nucl Cardiol Off Publ Am Soc Nucl Cardiol. 2013;20(5):860–70; quiz 857–9, 871–3.

29. Costa MA, Shoemaker S, Futamatsu H et al. Quantitative magnetic resonance perfusion imaging detects anatomic and physiologic coronary artery disease as measured by coronary angiography and fractional flow reserve. J Am Coll Cardiol. 2007;50(6):514–22.

30. Petersen SE, Jerosch-Herold M, Hudsmith LE et al. Evidence for microvascular dysfunction in hypertrophic cardiomyopathy: new insights from multiparametric magnetic resonance imaging. Circulation. 2007;115(18):2418–25.

31. Aquaro GD, Todiere G, Barison A et al. Myocardial blood flow and fibrosis in hypertrophic cardiomyopathy. J Card Fail. 2011;17(5):384–91.

Tables

Table 1 Baseline characteristics of normal subjects and type 2 diabetes mellitus patients

	T2DM pts., n=147	Normal controls, n=25
Age, yrs	58 (SD 12)	57 (SD 11)
Male, n (%)	106 (72)	17 (68)
Diabetes duration, yrs	12.9 (SD 8.1)	-
HbA1C, %	62.8 (SD 15.3)	34.6 (SD 2.8)
Body mass index, kg/m2	30.9 (SD 4.5)	25.1 (SD 3.3)
eGFR, ml/min/1.73m^2	81 (SD 14)	84 (SD 8)
Body mass index, kg/m2	30.9 (SD 4.5)	25.1 (SD 3.3)
Albumin:creatinine-ratio	127 (SD 423)	-
Retinopathy, n (%)	41 (28)	-
Peripheral neuropathy, n (%)	62 (42)	-
Systolic blood pressure, mmHg	136 (SD 17)	131 (SD 13)
Diastolic blood pressure, mmHg	81 (SD 11)	81 (SD 10)
Heart rate (rest), bpm	71 (SD 10)	60 (SD 8)
Heart rate (adenosine), bpm	92 (SD 14)	82 (SD 20)
Hypertension, n (%)	104 (70.7)	4 (16)
Ischemic heart disease, n (%)	18 (12.2)	0 (0%)
Medication, n (%)		
• Insulin	84 (57.1)	0 (0)
• GLP-1 agonist	54 (36.7)	0 (0)

• Metformin	124 (84.4)	0 (0)
• Statin	100 (68)	2 (8)
• ACEi/ARB	112 (76.2)	4 (16)
• SGLT2 inhibitor	53 (36.1)	0 (0)
LDL cholesterol, mean, mmol/L	2.1 (SD 0.88)	2.9 (SD 1.0)

Baseline characteristics of normal subjects and type 2 diabetes mellitus patients. SD (standard deviation), GLP-1 (glucagon like peptide 1), ACEi (angiotensin converting enzyme inhibitor), ARB (angiotensin receptor blocker), LDL (Low density lipoprotein). SGLT2 (Sodium glucose transport type 2 inhibitor)

Table 2 MRI parameters

	T2DM, n=147	Controls, n=25	*p value*
Myocardial blood flow (rest), ml/min/100g	81 (SD 19)	63 (SD 12)	p<0.0001*
Myocardial blood flow (adenosine), ml/min/100g	243 (SD 90)	311 (SD 82)	p=0.0003*
Myocardial blood flow increment from rest to stress, ml/min/100g	159 (SD 87)	249 (SD 80)	p<0.0001*
Myocardial perfusion reserve	3.06 (SD 1.11)	5.08 (SD 1.48)	p<0.0001*
Coronary sinus blood flow (rest), ml/min/100g	79 (SD 18)	71 (SD 18)	p=0.045*
Coronary sinus blood flow (adenosine), ml/min/100g	222 (SD 78)	336 (SD 57)	p<0.0001*
Coronary sinus blood flow increment from rest to stress, ml/min/100g	142 (SD 77)	265 (SD 57)	p<0.0001*
Coronary sinus perfusion reserve	2.86 (SD 1.03)	5.06 (SD 1.67)	p<0.0001*
Left ventricle myocardial mass, g	138 (SD 38)	121 (SD 25)	p=0.008*
Left ventricle end-systolic volume, ml	59 (SD 24)	63 (SD 15)	p=0.4
Left ventricle end-diastolic volume, ml	155 (SD 38)	165 (SD 39)	p=0.2

Values are mean values with standard deviation (SD). * p-values with significance level of 0.05.

Legends

Figure A

2 chamber steady-state free precession image showing a cross-section of the coronary sinus (arrow).

Figure B

Examples of coronary sinus blood flow curves during rest (dashed line) and adenosine stress (dotted line). In this patient, heart rate did not change with adenosine and hence the time-duration of the flow curves are equal. Please note the brief retrograde flow during initial systole, most notable with rest, and the more substantial forward flow during diastole. Flow is integrated over the entire duration of the heartbeat, and in this patient, coronary sinus flow increased about 3 fold (rest vs. adenosine stress: 61 vs. 184 ml/min; MPR = 3.02)

Figure C

Coronary sinus blood flow vs. myocardial blood flow (DCE) in 147 patients with type 2 diabetes mellitus (open) and 25 normal subjects (filled). Graph A: Flow measurements at rest, Graph B: Flow measurements at stress, Graph C: Increment flow values from rest to stress and Graph D: Stress-reserve values.

Figure D

Bland-Altman plots of the difference between myocardial blood flow (DCE) and coronary sinus blood flow (in percent) in 147 patients with type 2 diabetes mellitus (open) and 25 normal subjects (filled). Graph A: Flow measurements at rest, Graph B: Flow measurements at stress, Graph C: Increment flow values from rest to stress and Graph D: Stress-reserve values.

Figure E
Bland-Altman plots of the difference between myocardial blood flow (DCE) and coronary sinus blood flow (in percent) in 147 patients with type 2 diabetes mellitus. Graph A: Flow measurements at rest, Graph B: Flow measurements at stress, Graph C: Increment flow values from rest to stress and Graph D: Stress-reserve values.

Figure F
Bland-Altman plots of the difference between myocardial blood flow (DCE) and coronary sinus blood flow (in percent) in 25 healthy controls. Graph A: Flow measurements at rest, Graph B: Flow measurements at stress, Graph C: Increment flow values from rest to stress and Graph D: Stress-reserve values.

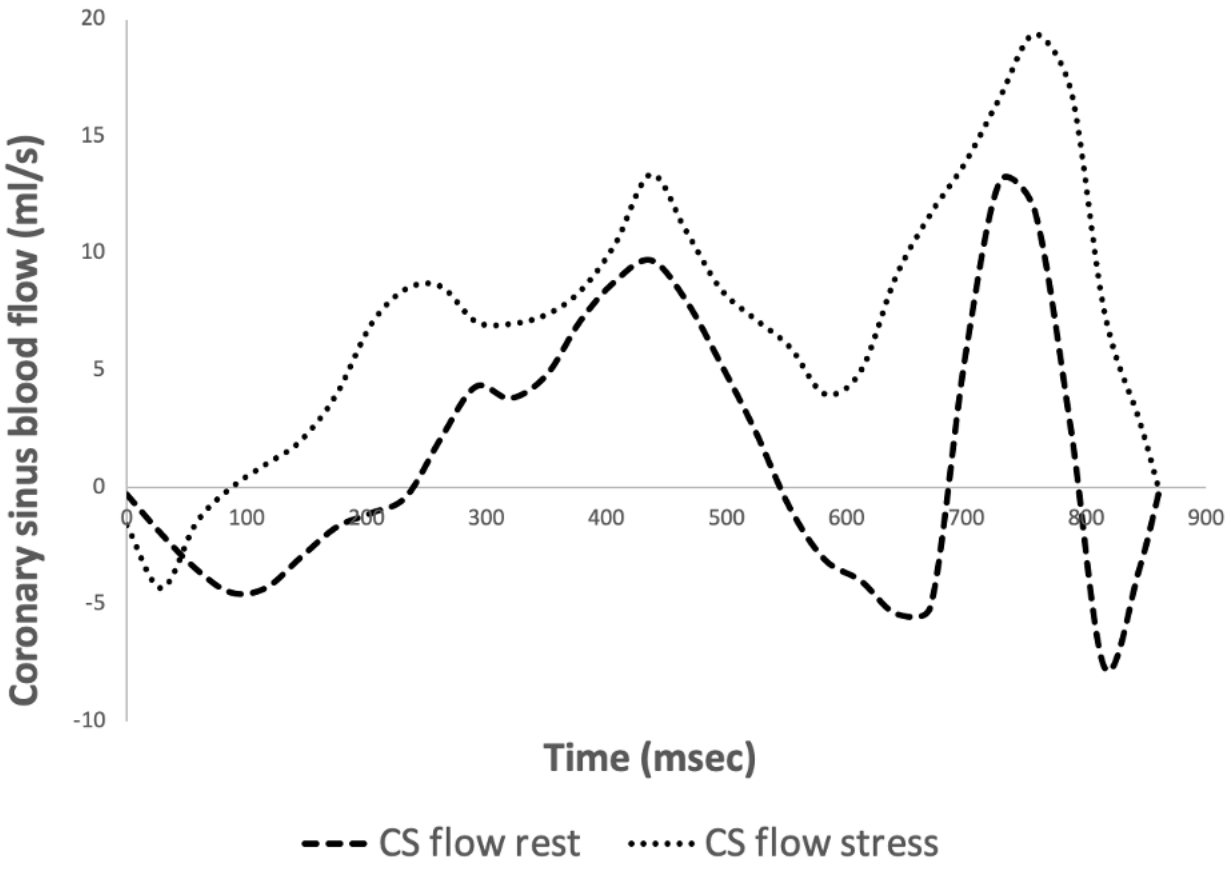

Fig B JMRI.tiff

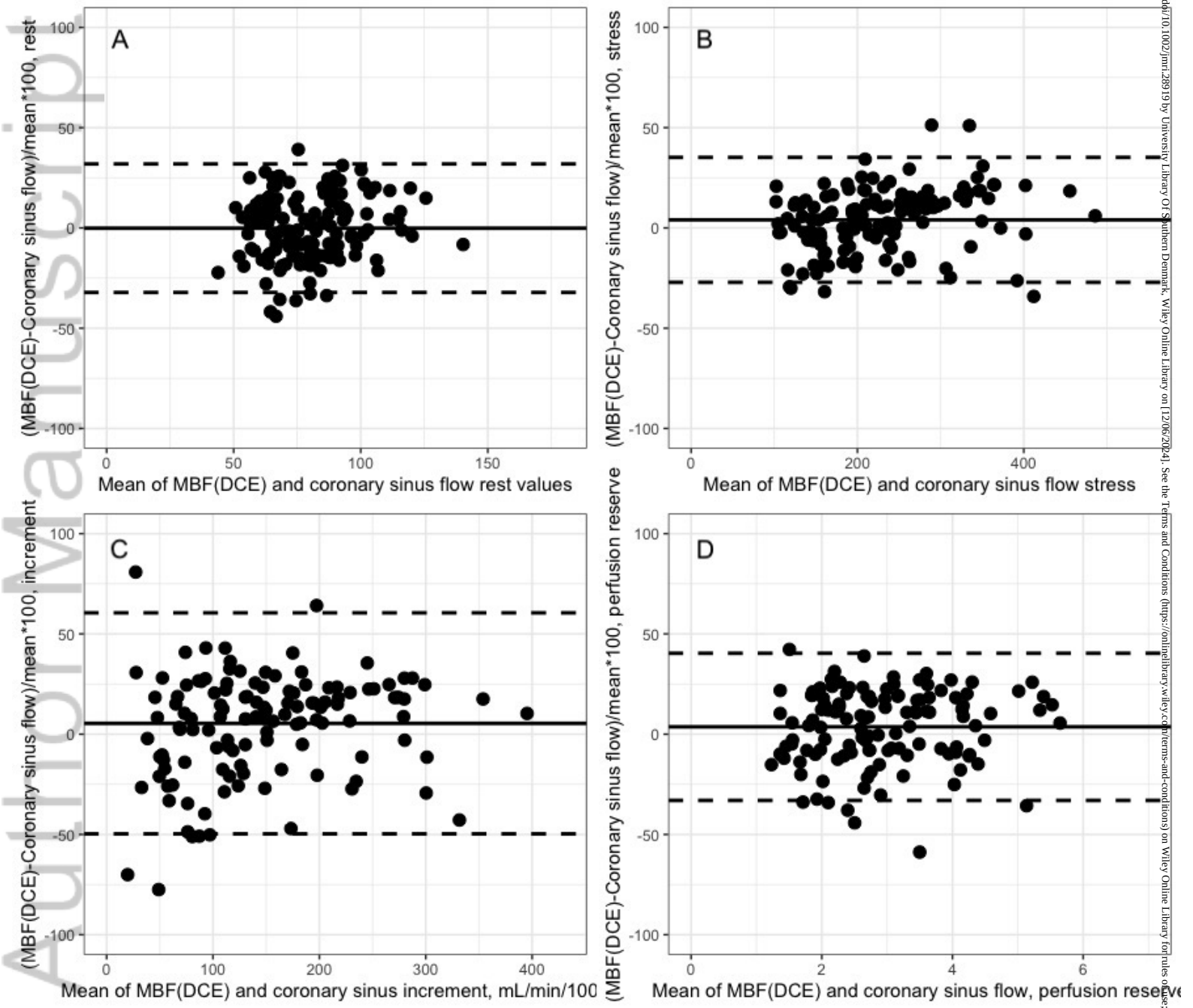

Fig E JMRI.tiff

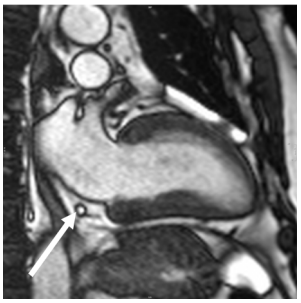

fig. A JMRI.tiff

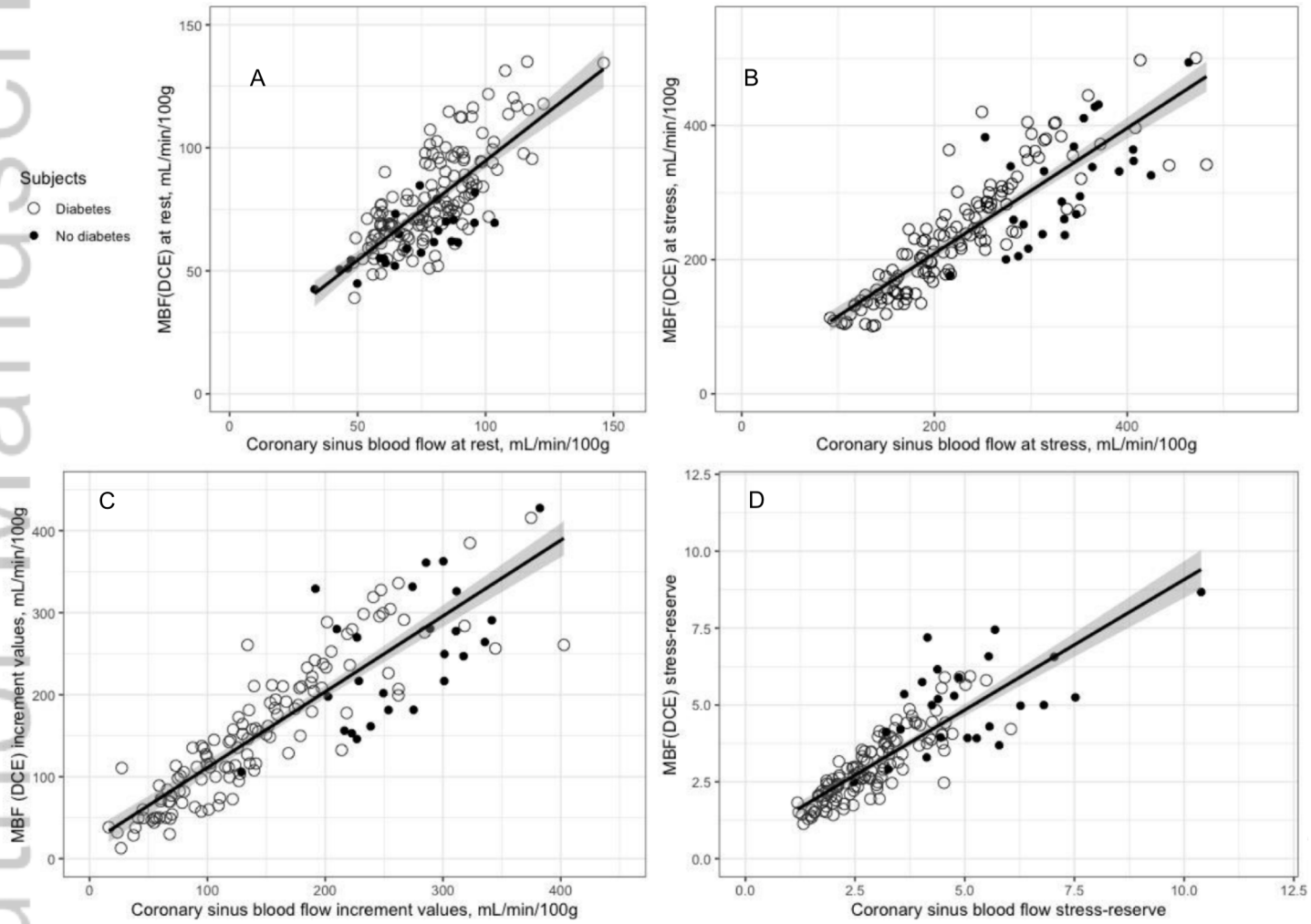

Fig. C JMRI.tiff

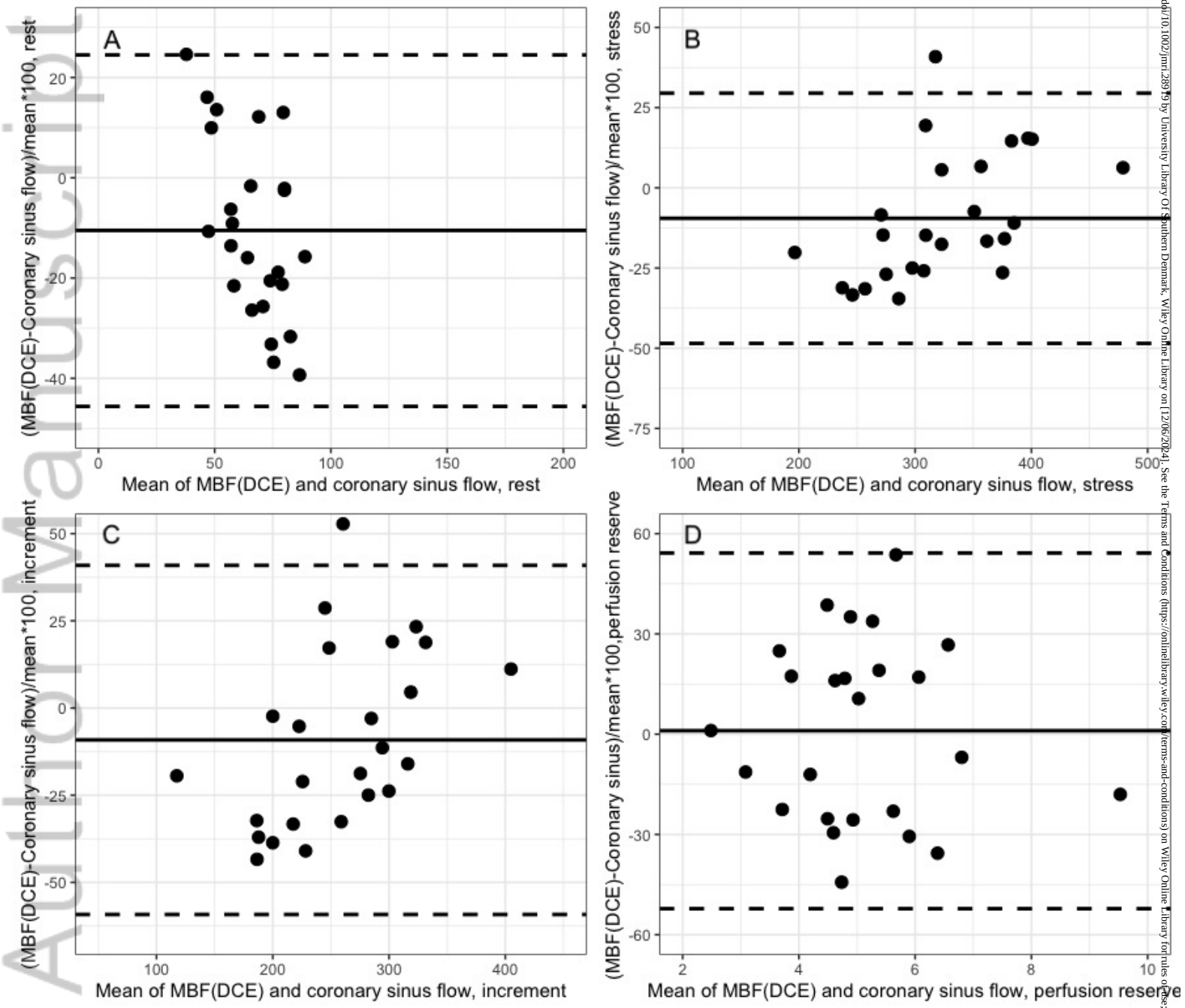

Fig. F JMRI.tiff

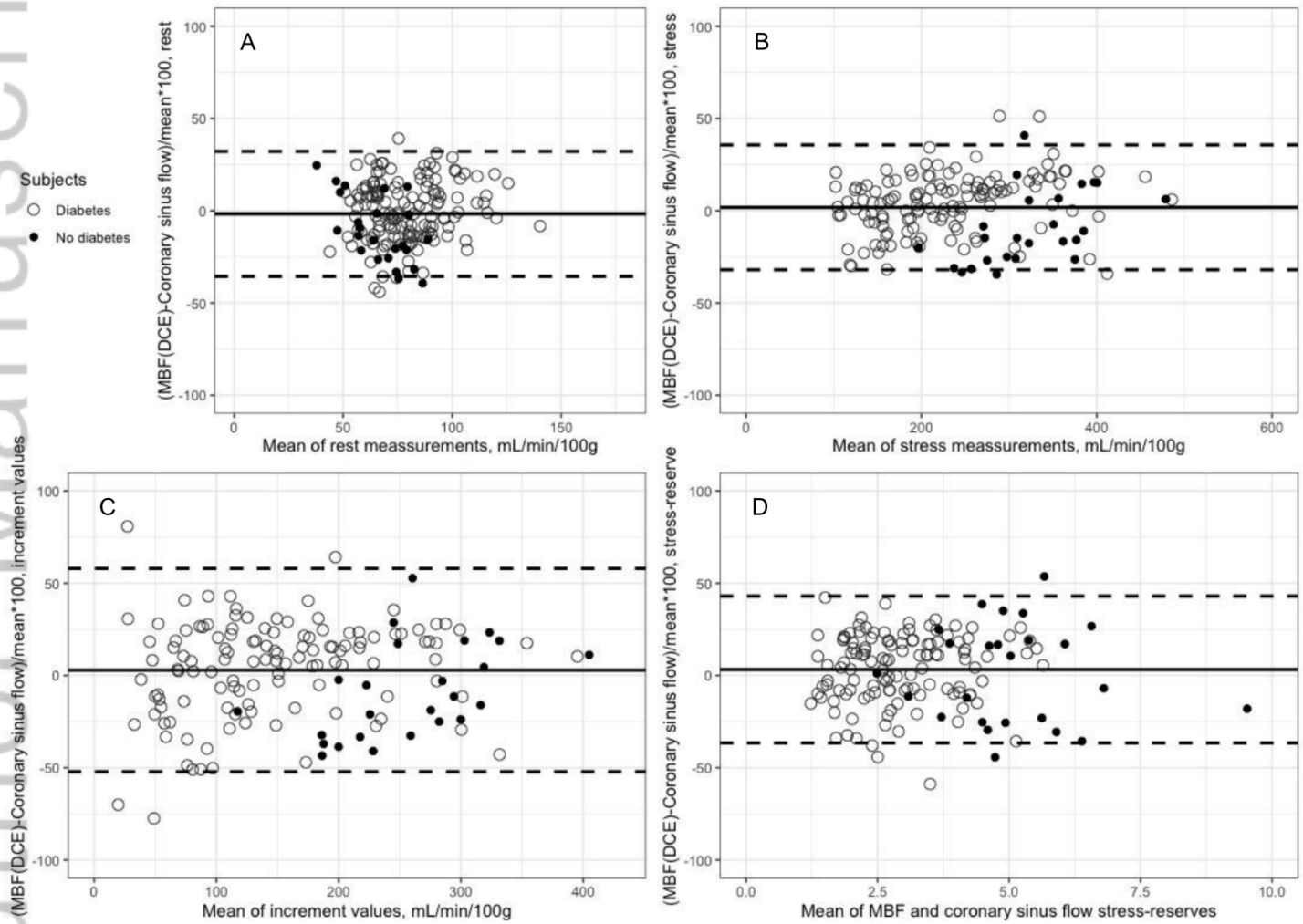

Fig.D JMRI.tiff